

Steady regime of radiation pressure acceleration with foil thickness adjustable within micrometers under 10-100 PW laser

Meng Liu,^{1,3} Wei-Min Wang,^{2,6,7,*} and Yu-Tong Li^{1,4,5,7,†}

¹*Beijing National Laboratory for Condensed Matter Physics,
Institute of Physics, CAS, Beijing 100190, China*

²*Department of Physics and Beijing Key Laboratory of Opto-electronic Functional Materials and Micro-nano Devices,
Renmin University of China, Beijing 100872, China*

³*Department of Mathematics and Physics, Noth China Electric Power university, Baoding, Hebei 071003, China*

⁴*School of Physical Sciences, University of Chinese Academy of Sciences, Beijing 100049, China*

⁵*Songshan Lake Materials Laboratory, Dongguan, Guangdong 523808, China*

⁶*Key Laboratory of Quantum State Construction and Manipulation (Ministry of Education),
Renmin University of China, Beijing, 100872, China*

⁷*IFSA Collaborative Innovation Center, Shanghai Jiao Tong University, Shanghai 200240, China
(Dated: May 11, 2023)*

Quasi-monoenergetic GeV-scale protons are predicted to efficiently generate via radiation pressure acceleration (RPA) when the foil thickness is matched with the laser intensity, e.g., L_{mat} at several nm to 100 nm with $10^{19} - 10^{22}$ Wcm⁻² available in laboratory. However, non-monoenergetic protons with much lower energies than prediction were usually observed in RPA experiments, because of too small foil thickness which is hard to bear insufficient laser contrast and foil surface roughness. Besides the technical problems, we here find that there is an upper-limit thickness L_{up} derived from the requirement that the laser energy density should dominate over the ion source, and L_{up} is lower than L_{mat} with the intensity below 10^{22} Wcm⁻², which causes inefficient or unsteady RPA. As the intensity is enhanced to $\geq 10^{23}$ Wcm⁻² provided by 10-100 PW laser facilities, L_{up} can significantly exceed L_{mat} and therefore RPA becomes efficient. In this regime, L_{mat} acts as a lower-limit thickness for efficient RPA, so the matching thickness can be extended to a continuous range from L_{mat} to L_{up} ; the range can reach micrometers, within which foil thickness is adjustable. This makes RPA steady and meanwhile the above technical problems can be overcome. Particle-in-cell simulation shows that multi-GeV quasi-monoenergetic proton beams can be steadily generated and the fluctuation of the energy peaks and the energy conversation efficiency remains stable although the thickness is taken in a larger range with increasing intensity. This work predicts that near future RPA experiments with 10-100 PW facilities will enter a new regime with the adjustable and large-range foil thickness for steady acceleration.

I. INTRODUCTION

Laser plasma interaction can provide approaches to realize compact ion accelerations due to high acceleration gradient [1–3]. The achieved ion beams with short bunch duration, compact size, and high density can be applied in fundamental science, plasma diagnostics and medical [1, 2, 4]. As one of the most attracting applications, tumor therapy [5, 6] demands proton beams with energy above 200 MeV and energy spread below 1% [1, 2]. Varieties of ion acceleration schemes have been proposed with the advancements in both high-power laser technology and targetry in the past two decades [7–15]. Among them, target normal sheath acceleration (TNSA) [16] is the predominant mechanism in most experiments of ion acceleration. TNSA demonstrated the cut-off proton energy near 100 MeV [11, 12], but the corresponding spectra are usually broad and the number at the cut-off energy is small. Radiation pressure acceleration (RPA) [17–20] is predicted to generate high-energy

quasi-monoenergetic ion beam with a sufficient number in the monoenergetic peak, which has potential to meet the demands in the key applications mentioned above.

However, RPA experiments usually achieved non-monoenergetic proton beams or quasi-monoenergetic peaks at much lower energies than theoretic predictions [21–23]. In RPA, the radiation pressure of an intense circularly-polarized (CP) laser pulse can push a substantial number of electrons forward, resulting in a strong charge-separation field for ion acceleration. When the radiation pressure is balanced with the charge-separation force, continuous ion acceleration can be obtained, which presents a matched foil thickness [2, 20]:

$$L_{mat} \simeq \frac{a_0 n_c \lambda}{\pi n_e}, \quad (1)$$

where $a_0 = (I_0 \lambda^2 / 2.74 \times 10^{18} \text{ Wcm}^{-2} \mu\text{m}^2)^{1/2}$ is the normalized laser amplitude, $n_c = m_e \omega^2 / 4\pi e^2$ is the critical density, and I_0 , ω and λ are the laser intensity, frequency, and wavelength, respectively. For $10^{19} - 10^{22}$ Wcm⁻² used in the existing RPA experiments [21, 24–28], L_{mat} is at a few nm to 100 nm. With such small thickness, the foil is easy to be deformed or broken by the amplified spontaneous emission (ASE) and prepulse of the

* weiminwang1@ruc.edu.cn

† ytli@iphy.ac.cn

high-power laser pulse[29, 30] before the main pulse interactions with the foil. Furthermore, according to the present target fabrication technology, the surface roughness is typically at the same order with such thickness. These limitations in the current target and laser technology tend to result in inefficiency and unsteadiness of RPA, which could become worse due to transverse instabilities [31–33] and plasma heating [34].

Besides the above factors, we find here that there is an upper-limit thickness L_{up} for efficient RPA and L_{up} is lower than or around L_{mat} with the intensity below 10^{22} Wcm $^{-2}$ ($a_0 = 61$) adopted in reported experiments[21, 24–26], which could cause inefficient or unsteady acceleration. As the intensity is enhanced to 10^{23} Wcm $^{-2}$ available recently[35], L_{up} starts to significantly exceed L_{mat} , resulting in that the matching thickness can be extended to a large range from L_{mat} to L_{up} and up to several micrometers. This can bring both efficient and steady RPA and meanwhile the above technical problems can be overcome. In this regime, multi-GeV quasi-monoenergetic proton beams can be steadily generated and the fluctuation of the energy peaks and the energy conversation efficiency remains stable although the thickness is taken in a larger range with increasing intensity.

II. THE UPPER-LIMIT THICKNESS FOR STEADY RPA

For the efficient and steady RPA, the requirement that the driving laser energy density should dominate over the ion source within the laser focal spot gives the upper-limit thickness:

$$L_{up} \leq \frac{W_R \sqrt{1 - v_i^2/c^2}}{\pi R^2 n_i m_i c^2}, \quad (2)$$

so that the laser pulse has enough surplus energy to transform to the ions kinetic energy, independent of the acceleration process. Here W_R is the laser energy within the focal spot radius R , n_i is the initial ion density, and $m_i c^2$ is the ion rest energy. We estimate the ion velocity v_i as v_g or $2v_p/(1 + v_p^2)$, where v_g is the relativistic group velocity of laser [15, 36], $v_p = \sqrt{\Pi}/(1 + \sqrt{\Pi})$ is the piston velocity in the relativistic case [17, 36–38], and $\Pi = 2a_0^2 Z n_c m_e / (A n_e m_i)$, Z/A is the charge-mass ratio, and m_i is the ion mass. Our simulation below will show that they are two typical velocities in "hole-boring" [18, 39] and "light-sail" [14, 15, 40–42] phases in ion acceleration, respectively.

According to Eqs. (1) and (2) with a given density $n_e = 200n_c$, $L_{up} = L_{mat} = 0.196\lambda$ when $a_0 = 122$ (corresponding to 4×10^{22} Wcm $^{-2}$); and $L_{up} > L_{mat}$ always holds for $a_0 > 122$, as shown in Fig. 1(a). Note that the intensities below and far below 4×10^{22} Wcm $^{-2}$ were adopted in existing PRA experiments[21, 25, 26]. Therefore, unsteady experimental results are not only

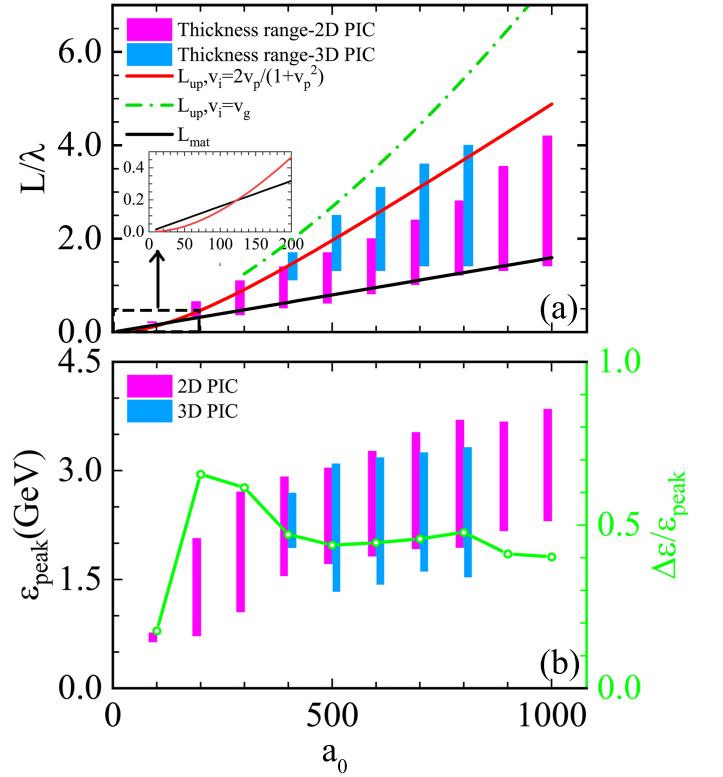


FIG. 1. (a) The target thickness L for efficient RPA as a function of the laser amplitude a_0 , where the pink-splines and blue-splines correspond 2D and 3D PIC results, respectively, the black line is L_{mat} calculated from Eq.(1), and the red and green-dashed lines show L_{up} calculated from Eq.(2) with v_i estimated as $2v_p/(1 + v_p^2)$ and v_g , respectively. The target thickness for efficient RPA is counted when a quasi-monoenergetic proton beam is generated in PIC simulation. (b) The corresponding energy peaks ϵ_{peak} of the quasi-monoenergetic proton beams are displayed by pink-splines and blue-splines for 2D and 3D PIC results, respectively. The green line with circles is the fluctuation of the peak energies $\Delta\epsilon/\epsilon_{peak}$ obtained from the 2D-PIC simulations.

because of the too small thickness L_{mat} with low tolerance to the insufficient laser contrast and foil surface roughness, but also because of the requirement that the driving laser energy density should dominate over the ion source, i.e., the thickness L should be less than L_{up} . Adopting L as L_{mat} for efficient RPA has been widely recognized, so the requirement of $L_{up} > L$ is roughly equivalent to $L_{up} > L_{mat}$. As the laser intensity is higher than 4×10^{22} Wcm $^{-2}$, an efficient RPA with $L_{up} > L_{mat}$ starts to be possible. Further, to achieve a steady RPA, L_{up} should be much greater than L_{mat} and then the thickness can be chosen in a large range. For example, when $a_0 = 300$ (corresponding to 2.47×10^{23} Wcm $^{-2}$), $L_{up} = 0.91\lambda$ and $L_{mat} = 0.48\lambda$ and in principle, the thickness can be taken in a range from 0.48λ to 0.91λ . For higher laser intensity, the thickness range $\Delta L = L_{up} - L_{mat}$ is enlarged further, which can be observed in Fig. 1(a) and also explained in the follow-

ing. One can easily derive $L_{up} \propto \xi^2 \sqrt{1 + 2\alpha_0 \xi} / (1 + \alpha_0 \xi)$ and $L_{mat} \propto \xi \sqrt{n_c/n_e}$, where $\alpha_0 = \sqrt{2} Z m_e / (A m_i)$ and $\xi = a_0 \sqrt{n_c/n_e}$ (see Supplementary Eqs. (S5) and (S8)). For a given n_e or foil species, L_{up} increases more quickly than L_{mat} with the growth of a_0 , i.e., the thickness range ΔL is enlarged continuously. These analytical results are verified by our particle-in-cell (PIC) simulation results shown by the pink- and blue-splines in Fig. 1(a).

III. PIC SIMULATION RESULTS

We perform two-dimensional (2D) and three-dimensional (3D) PIC simulations by the EPOCH code [43]. A CP laser pulse with a wavelength $\lambda = 1 \mu\text{m}$ and an intensity profile of $I_0 \exp(-2t^2/\tau^2) \exp(-y^4/R^4)$ is incident along the x direction, where the spot radius is $R = 6\lambda$ and the duration is 30 fs. The pulse arrives at the vacuum-foil interface $x = 15\lambda$ at $t = 0$. The foil is composed of protons H^+ and e^- with $n_e = 200n_c$. We take a simulation box $40\lambda \times 50\lambda$ (4000×2500 cells in $x \times y$) moving along the x direction at the speed of light and each cell has 100 macro-particles in foil region.

Fig. 1(a) shows the target thickness for efficient RPA as a function of a_0 , where the pink-splines and blue-splines correspond 2D and 3D PIC results, respectively. For a given a_0 , we change the foil thickness and count the thickness value with which a quasi-monoenergetic GeV proton beam is generated. The counted values are illustrated by a spline representing an adjustable thickness range. One can see that the range is enlarged with the growth of a_0 and the pink-splines fall well between the black and red lines, in good agreement with Eq. (1) and Eq. (2). This suggests that there is indeed an upper-limit thickness for efficient RPA, set by the requirement of the driver energy density dominating over the source energy density.

The PIC results also indicate that: the well-known matching thickness L_{mat} acts as a lower-limit value for efficient RPA, and then the matching thickness originally as an isolated value point can be extended to a continuous range. This is because L_{mat} is derived under an ideal condition that the foil electrons as a whole is pushed forward and form charge-separation field to balance with the laser radiation pressure exerted on the electrons. Actually, only part of the foil electrons can be pushed forward out of the foil, which is becomes more significant for a relatively large thickness with high laser intensity. Furthermore, the electrostatic force of charge-separation field $E_x = 4\pi e n_e L$ should be higher than the radiation pressure $2I/c$. Otherwise, the foil electrons can be blown out, the compressed electron layer cannot be formed, and ions cannot be accelerated. Hence,

$$L \geq L_{mat}, \quad (3)$$

should be a more reasonable condition for sustaining the charge-separation field to accelerate ions continuously. It should be noted that Eqs. (1) and (2) are given in the

1D case. The omitted transverse effects tend to deteriorate the target and a thicker foil is needed to overcome the deterioration. Thus, 2D PIC results are in better agreement with L_{mat} and L_{up} than 3D ones.

The enlarged efficient thickness range bounded by L_{mat} and L_{up} provides a favorable freedom for foil thickness choice and the matched thickness can be adopted as a value much higher than the original prediction by L_{mat} . For instance, quasi-monoenergetic GeV proton beams can be stably generated from the foil with a thickness within $0.4\lambda - 1.2\lambda$ for $a_0 = 300$, and $0.8\lambda - 2.1\lambda$ for $a_0 = 600$ from PIC results (also see Supplementary Note 1 and Fig. S2). When $a_0 \geq 1000$, the thickness range ΔL even enlarges above 2λ , favoring the target design in future experiments.

Although the thickness is taken in a larger range with increasing a_0 , the fluctuation of the energy peaks remains stable, as shown in Fig. 1(b). This figure plots the energy peaks ε_{peak} of the quasi-monoenergetic proton beams obtained from 2D and 3D PIC results. In the typical simulation with $a_0 = 300$, the peak energy decreases from 3.6 GeV to 1.2 GeV as the foil thickness increases from 0.4λ to 1.2λ . With a larger amplitude $a_0 = 600$, the peak energy only decreases from 4.5 GeV to 3.0 GeV as the foil thickness increases from 0.8λ to 2.1λ (also see Supplementary Note 1 and Fig. S2). The green line in Fig. 1(b) displays the energy fluctuation $\Delta\varepsilon/\varepsilon_{peak}$ as a function of a_0 . It is shown that the fluctuation reaches 70% at $a_0 = 200$, decreases to 40% at $a_0 = 400$, and then maintains around this value since $a_0 \geq 400$. Even the thickness range ΔL is above 2λ with $a_0 \geq 1000$, $\Delta\varepsilon/\varepsilon_{peak}$ does not grow. This is because the proton velocity or peak energy is mainly determined by the laser relativistic group velocity which increases slowly with the growing a_0 when a_0 is sufficiently large. The slowly increasing group velocity also causes that the energy conversion efficiency of the protons basically remains around 20% – 25% as shown in the Supplementary Note 2, Fig. S4 and Table S1.

Fig. 2 shows the evolution of tracked proton velocity v_i and the laser wavefront velocity v_f representing the group velocity, where v_f is defined as the moving velocity of the laser intensity surface $I_0/10$ and I_0 is the initial intensity. The evolution of v_f can be separated into two stages in Fig. 2(b)-(d). In the first stage with $t \lesssim 11 - 12T_0$, v_f firstly decreases dramatically at the beginning interaction of the laser with the foil, and later increases quickly along with the foil being pushed forward by laser radiation pressure. This stage has been widely studied[18, 38] and v_i can be estimated as $2v_p/(1 + v_p^2)$. At the second stage after about $12T_0$, v_f becomes roughly constant and v_i is very close to v_f in Figs. 2(b)-2(d) with $a_0 = 300 - 700$, meaning that the protons are efficiently and continuously accelerated and then move along with the laser pulse. In this stage, v_i can be estimated by the relativistic group velocity v_g [15, 31, 44], where $v_i \simeq 0.973c$ and $v_i \simeq 0.982c$ for the cases with $a_0 = 500$ and $a_0 = 700$ read from Fig. 2(c) and 2(d). In this case,

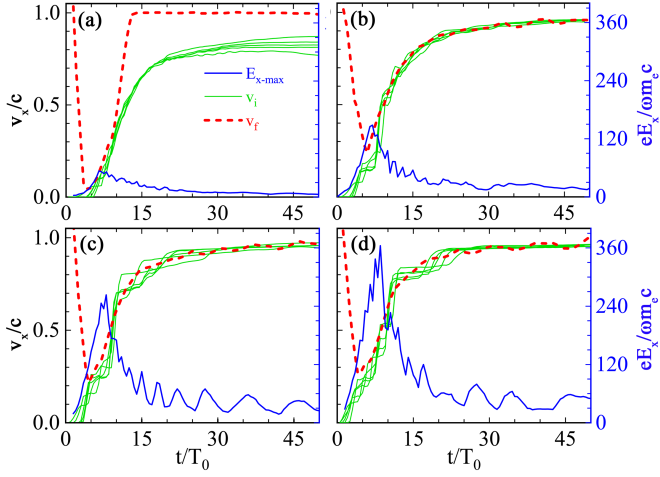


FIG. 2. Temporal evolution of the laser wavefront velocity v_f (red dotted-line) and tracked proton velocity v_i (green-line), where we track 100 protons gaining high energies finally and take 5 typical ones. Evolution of the maximum of the longitudinal electric field E_{x-max} (corresponding to the right y -axis) is also displayed by the blue line. Here the laser amplitude a_0 and target thickness L are taken as (100, 0.18 λ), (300, 0.56 λ), (500, 1.1 λ) and (700, 1.7 λ) in (a)-(d), respectively.

the group velocity $v_g/c \simeq 1 - \frac{n_e}{\sqrt{2}a_0 n_c}$ grows slowly with a_0 ($a_0 \gg 1$). This agrees with Fig. 1(b) that the peak energy increases slowly from $a_0 = 400$ to $a_0 = 1000$. By contrast, in Fig. 2(a) with $a_0 = 100$, the protons velocity can only reach 0.75 c much lower than v_f because the laser wavefront breaks through the foil and the protons cannot catch up.

Fig. 3 shows that the plasma heating is suppressed with the growing laser intensity, facilitating the acceleration. Compared with the case with $a_0 = 100$, the plasma temperature is reduced by 50% with $a_0 = 300$ and 75% with $a_0 = 500$ and 700 at the second stage. In efficient RPA with the high intensities, the protons and electrons move along with the laser pulse and then their velocities [see Fig. 2(b)-(d)] are close c and mainly in the longitudinal direction, i.e., most of the particle energies are longitudinal, among which the protons cover most energies. This causes significant reductions of the temperature and the transverse spread of electrons.

The upper-limit thickness L_{up} in Eq. (2) is given by the requirement that the driving laser energy density should dominate over the proton source within the laser focal spot during the efficient RPA. The requirement is verified by Fig. 4, which displays the energy densities of the protons and the laser. When the thickness is in the range from L_{mat} to L_{up} for the efficient RPA, e.g., Figs. 4(b)-(d), the laser energy density is dominant over the proton energy density. Fig. 4(e) illustrates the evolution of the energy density ratio Γ of the protons to the laser. Γ is less than 1 in the whole simulation duration for $(a_0, L) = (500, 1.1\lambda)$ and $(700, 1.7\lambda)$ and before $t = 30T_0$ for

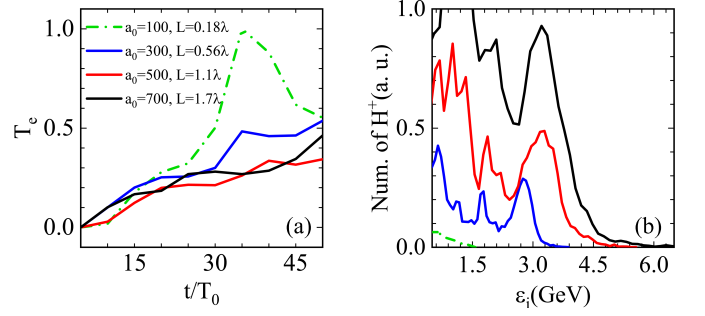


FIG. 3. (a) Evolution of the plasma electron temperature and (b) the energy spectra of protons at $t = 70T_0$, where different lines in (a) and (b) represent different (a_0, L) corresponding to the parameters taken in Figs. 2(a)-2(d), respectively. The plasma temperature are calculated with the electrons in the compressed density layer and normalized by that in the case of $a_0 = 100$.

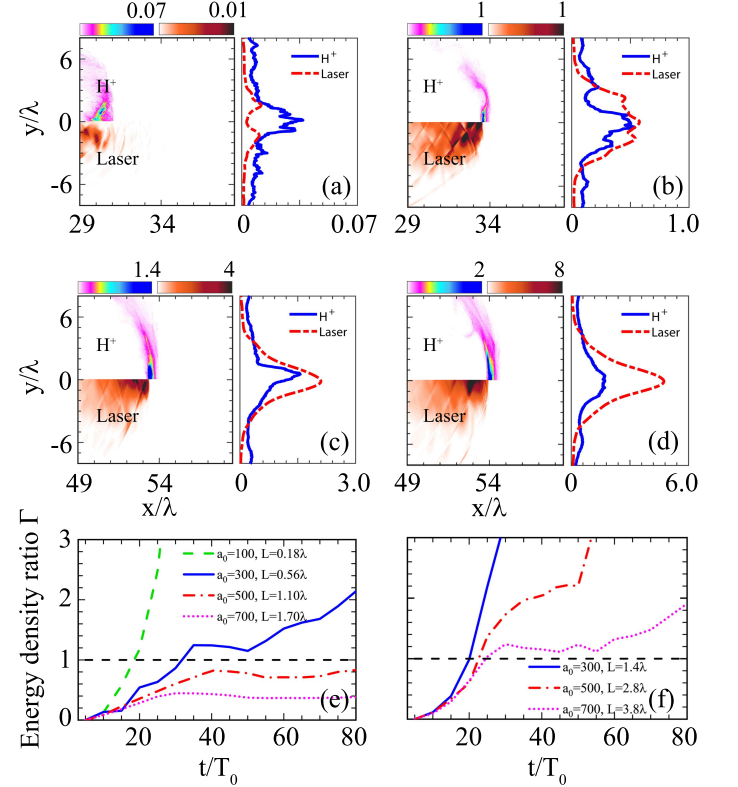


FIG. 4. (a)-(d) Spatial distributions of energy densities of the protons (top half) and the laser (bottom half) and the energy densities integrated along x versus y are also plotted by curves, where (a) and (b) are the cases with $a_0 = 100/300$ at $t = 30T_0$ and (c) and (d) are the cases with $a_0 = 500/700$ at $t = 50T_0$. [(e), (f)] Temporal evolution of the energy density ratio between the protons and the laser, where the ratio is calculated by the energy density peaks of the protons and the laser.

(300, 0.56λ) [also see Fig. 4(b) given at $t = 30T_0$], which corresponds to the efficient acceleration time. While the thickness is larger than L_{up} for the given $a_0=300, 500,$ and $700,$ shown in Fig. 4(f), Γ starts to be more than 1 as early as about $t = 20T_0$ and the acceleration is inefficient (i.e., no quasi-monoenergetic peak or much lower peak energy).

IV. CONCLUSION AND DISCUSSION

In summary, we have found there is an upper-limit thickness L_{up} for efficient RPA, deriving from the requirement that the driving laser energy density should dominate over the proton source. The well-known matching thickness L_{mat} acts as a lower-limit value, and therefore, the matching thickness originally as an isolated value point can be extended to a continuous range from L_{mat} to L_{up} . $L_{up} > L_{mat}$ can be achieved for steady RPA with $I_0 > 4 \times 10^{22}$ Wcm $^{-2}$ and the thickness range $L_{up} - L_{mat}$ is enlarged with the laser intensity. For $10^{23} \sim 10^{24}$ Wcm $^{-2}$ delivered from the 10 PW and 100 PW laser facilities[51–53], the thickness range can reach a few micrometers providing favorable freedom for foil thickness choice in RPA experiments. Although the thickness is taken in an larger range with increasing intensity, the fluctuation of the energy peaks as well as the energy conversion efficiency remains stable. This work predicts that near future RPA experiments with 10-100 PW laser facilities will enter a new regime with the adjustable and large-range target thickness for steady ion acceleration.

Note that in Eq. (2) the proton velocity v_i is mainly estimated by the laser relativistic group velocity v_g , which has been verified by Fig. 2, and the laser energy is

calculated with the spot radius at the focusing plane, which does not change significantly with laser propagation within the Rayleigh length ($113 \mu\text{m}$ in our case). Therefore, Eq. (2) can give a reasonable L_{up} close to the PIC simulations.

We also check the influence of the strong field quantum electrodynamics (QED) effects [45–48] on RPA. The influence enhances with the growing a_0 , but basically it can be negligible (see Supplementary Note 3 and Fig. S5). With $a_0 = 1000$, the energy conversion efficiency of the gamma-photons increases with the target thickness and it reaches 8% at the maximum thickness 4.4λ for efficient RPA, where both the energy peak and energy conversion of the protons are reduced by less than 6%. In efficient RPA, electrons move mainly along the laser propagating direction which makes small QED parameters and weak QED effects [48, 49].

Besides the foil species composed of $n_H = n_e = 200n_c$, we also investigated the steady RPA process for the lower density with $n_H = n_e = 100n_c$ (see Supplementary Table S1). Moreover, the realistic targets, lithium hydride(LiH)[50] with different thicknesses, are also adopted and the results agree with Eq (2)(see Supplementary Note 4 and Fig. S6).

ACKNOWLEDGMENTS

This work was supported by the National Key R&D Program of China (Grant No. 2018YFA0404801), National Natural Science Foundation of China (Grants No. 12205366), the Strategic Priority Research Program of Chinese Academy of Sciences (Grant Nos. XDA25050300, XDA25010300), and the Fundamental Research Funds for the Central Universities (Grant Nos. 2020MS138).

-
- [1] H. Daido, M. Nishiuchi and A. S. Pirozhkov, "Review of laser-driven ion sources and their applications," Rep. Prog. Phys. **75**, 056401 (2012).
 - [2] A. Macchi, M. Borghesi and M. Passoni, "Ion acceleration by superintense laser-plasma interaction." Rev. Mod. Phys. **85**, 751 (2013).
 - [3] J. Fuchs, P. Antici, E. d'Humières, E. Lefebvre, M. Borghesi, E. Brambrink, C. A. Cecchetti, M. Kaluza, V. Malka, M. Manclossi, S. Meyroneinc, P. Mora, J. Schreiber, T. Toncian, H. Pépin and P. Audebert, "Laser-driven proton scaling laws and new paths towards energy increase," Nat. phys. **2**, 48-54 (2005).
 - [4] M. Roth, T. E. Cowan, M. H. Key, S. P. Hatchett, C. Brown, W. Fountain, J. Johnson, D. M. Pennington, R. A. Snavely, S. C. Wilks, K. Yasuike, H. Ruhl, F. Pegoraro, S. V. Bulanov, E. M. Campbell, M. D. Perry and H. Powell, "Fast ignition by intense laser-accelerated proton beams," Phys. Rev. Letts. **86**, 436 (2001).
 - [5] U. Linz and J. Alonso, "What will it take for laser driven proton accelerators to be applied to tumor therapy," Rev. Accel. Beams **10**, 094801 (2007).
 - [6] S. V. Bulanov, T. Z. Esirkepov, V. S. Khoroshkov, A. V. Kuznetsov and F. Pegoraro, "Oncological hadrontherapy with laser ion accelerators," Phys. Lett. A.**299**, 240 (2002).
 - [7] R. A. Snavely, M. H. Key, S. P. Hatchett, T. E. Cowan, M. Roth, T. W. Phillips, M. A. Stoyer, E. A. Henry, T. C. Sangster, M. S. Singh, S. C. Wilks, A. MacKinnon, A. Offenberger, D. M. Pennington, K. Yasuike, A. B. Langdon, B. F. Lasinski, J. Johnson, M. D. Perry, and E. M. Campbell, "Intense high-energy proton beams from petawatt-laser irradiation of solids," Phys. Rev. Letts. **85**, 2945 (2000).
 - [8] L. L. Ji, B. F. Shen, X. M. Zhang, F. C. Wang, Z. Y. Jin, X. M. Li, M. Wen and J. R. Cary, "Generation monoenergetic heavy-ion bunches with laser-induced electrostatic shocks," Phys. Rev. Lett. **101**, 164802 (2008).
 - [9] A. X. Li, C. Y. Qin, H. Zhang, S. Li, L. L. Fan, Q. S. Wang, T. J. Xu, N. W. Wang, L. H. Yu, Y. Xu, Y. Q. Liu, C. Wang, X. L. Wang, Z. X. Zhang, X. Y. Liu, P. L.

- Bai, Z. B. Gan, X. B. Zhang, X. B. Wang, C. Fan, Y. J. Sun, Y. H. Tang, B. Yao, X. Y. Liang, Y. X. Leng, B. F. Shen, L. L. Ji, R. X. Li, and Z. Z. Xu, "Acceleration of 60 MeV proton beams in the commissioning experiment of the SULF-10 PW laser," *High Power Laser Sci. Eng.* **10**, 0400e26 (2022).
- [10] D. Haberberger, S. Tochitsky, F. Fiuza, C. Gong, R. A. Fonseca, L. O. Silva, W. B. Mori and C. Joshi, "Collisionless shocks in laser-produced plasma generate monoenergetic high-energy proton beams," *Nat. Phys.* **8**, 95-99 (2012).
- [11] F. Wagner, O. Deppert, C. Brabetz, P. Fiala, A. Kleinschmidt, P. Poth, V. A. Schanz, A. Tebartz, B. Zielbauer, M. Roth, T. Stöhlker and V. Bagnoud, "Maximum Proton Energy above 85 MeV from the Relativistic Interaction of Laser Pulses with Micrometer Thick CH₂ Targets," *Phys. Rev. Letts.* **116**, 205002 (2016).
- [12] A. Higginson, R. J. Gray, M. King, R. J. Dance, S. D. R. Williamson, N. M. H. Butler, R. Wilson, R. Capdessus, C. Armstrong, J. S. Green, S. J. Hawkes, P. Martin, W. Q. Wei, S. R. Mirfayzi, X. H. Yuan, S. Kar, M. Borghesi, R. J. Clarke, D. Neely and P. McKenna, "Near-100 MeV protons via a laser-driven transparency-enhanced hybrid acceleration scheme," *Nat. Commun.* **99**, 724 (2018).
- [13] N. P. Dover, M. Nishiuchi, H. Sakaki, K. Kondo, M. A. Alkhimova, A. Ya Faenov, M. Hata, N. Iwata, H. Kiriyama, J. K. Koga, T. Miyahara, T. A. Pikuz, A. S. Pirozhkov, A. Sagisaka, Y. Sentoku, Y. Watanabe, M. Kando and K. Kondo, "Effect of small focus on electron heating and proton acceleration in ultrarelativistic laser-solid interactions," *Phys. Rev. Letts.* **124**, 084802 (2020).
- [14] A. Macchi, S. Veghini, T. V. Liseykina and F. Pegoraro, "Radiation pressure acceleration of ultrathin foils," *New J. Phys.* **12**, 045013 (2010).
- [15] S. S. Bulanov, E. Esarey, C. B. Schroeder, S. V. Bulanov, T. Zh. Esirkepov, M. Kando, F. Pegoraro and W. P. Leemans, "Enhancement of maximum attainable ion energy in the radiation pressure acceleration regime using a guiding structure," *Phys. Rev. Lett.* **114**, 105003 (2015).
- [16] S. C. Wilks, A. B. Langdon, T. E. Cowan, M. Roth, M. Singh, S. Hatchett, M. H. Key, D. Pennington, A. MacKinnon and R. A. Snavely, "Energetic proton generation in ultra-intense laser-solid interactions," *Phys Plasmas.* **8**, 542 (2001).
- [17] T. Esirkepov, M. Borghesi, S. V. Bulanov, G. Mourou and T. Tajima, "Highly efficient relativistic ion generation in the laser-piston regime," *Phys. Rev. Lett.* **92**, 175003 (2004).
- [18] A. Macchi, F. Cattani, T. V. Liseykina and F. Cornolti, "Laser acceleration of ion bunches at the front surface of overdense plasmas," *Phys. Rev. Lett.* **94**, 165003 (2005).
- [19] A. P. L. Robinson, M. Zepf, S. Kar, R. G. Evans and C. Bellei, "Radiation pressure acceleration of thin foils with circularly polarized laser pulses," *New. J. Phys.* **10**, 013021 (2008).
- [20] X. Q. Yan, C. Lin, Z. M. Sheng, Z. Y. Sheng, Z. Y. Guo, B. C. Liu, Y. R. Lu, J. X. Fang and J. E. Chen, "Generating High-Current Monoenergetic Proton Beams by a Circularly Polarized Laser Pulse in the Phase-Stable Acceleration Regime," *Phys. Rev. Lett.* **100**, 135003 (2008).
- [21] A. Henig, S. Steinke, M. Schünrer, T. Sokollik, R. Hörlein, D. Kiefer, D. Jung, J. Schreiber, B. M. Hegelich, X. Q. Yan, J. Meyer-ter-Vehn, T. Tajima, P. V. Nickles, W. Sandner and D. Habs, "Radiation-pressure acceleration of ion beams driven by circularly polarized laser pulses," *Phys. Rev. Lett.* **103**, 245003 (2009).
- [22] D. Jung, L. Yin, B. J. Albright, D. C. Gautier, R. Hörlein, D. Kiefer, A. Henig, R. Johnson, S. Letzring, S. Palaniyappan, R. Shah, T. Shimada, X. Q. Yan, K. J. Bowers, T. Tajima, J. C. Fernández, D. Habs and B. M. Hegelich, "Monoenergetic ion beam generation by driving ion solitary waves with circularly polarized laser light," *Phys. Rev. Lett.*, **107**, 115002 (2011).
- [23] F. Dollar, C. Zwick, A. G. R. Thomas, V. Chvykov, J. Davis, G. Kalinchenko, T. Matsuoka, C. McGuffey, G. M. Petrov, L. Willingale, V. Yanovsky, A. Maksimchuk and K. Krushelnick, "Finite spot effects on radiation pressure acceleration from intense high-contrast laser interactions with thin targets," *Phys. Rev. Lett.* **108**, 175005 (2012).
- [24] S. Kar, K. F. Kakolee, B. Qiao, A. Macchi, M. Cerchez, D. Doria, M. Geissler, P. McKenna, D. Neely, J. Osterholz, R. Prasad, K. Quinn, B. Ramakrishna, G. Sarri, O. Willi, X. Y. Yuan, M. Zepf and M. Borghesi, "Ion acceleration in multispecies targets driven by intense laser radiation pressure," *Phys. Rev. Lett.*, **109**, 185006 (2012).
- [25] I. J. Kim, K. H. Pae, H. W. Choi, C. L. Lee, H. T. Kim, H. Singhal, J. H. Sung, S. K. Lee, H. W. Lee, P. V. Nickles, T. M. Jeong, C. M. Kim and C. H. Nam, "Radiation pressure acceleration of protons to 93 MeV with circularly polarized petawatt laser pulses," *Phys. Plasmas* **23**, 070701 (2016).
- [26] W. J. Ma, I. J. Kim, J. Q. Yu, H. W. Choi, P. K. Singh, H. W. Lee, J. H. Sung, S. K. Lee, C. Lin, Q. Liao, J. G. Zhu, H. Y. Lu, B. Liu, H. Y. Wang, R. F. Xu, X. T. He, J. E. Chen, M. Zepf, J. Schreiber, X. Q. Yan and C. H. Nam, "Laser acceleration of highly energetic carbon ions using a double-layer target composed of slightly underdense plasma and ultrathin foil," *Phys. Rev. Letts.* **122**, 014803 (2019).
- [27] A. Alejo, H. Ahmed, A. G. Krygier, R. Clarke, R. R. Freeman, J. Fuchs, A. Green, J. S. Green, D. Jung, A. Kleinschmidt, J. T. Morrison, Z. Najmudin, H. Nakamura, P. Norreys, M. Notley, M. Oliver, M. Roth, L. Vassura, M. Zepf, M. Borghesi and S. Kar, "Stabilized radiation pressure acceleration and neutron generation in ultrathin deuterated foils," *Phys. Rev. Lett.* **129**, 114801 (2022).
- [28] Y. Kuramitsu, T. Minami, T. Hihara, K. Sakai, T. Nishimoto, S. Isayama, Y. T. Liao, K. T. Wu, W. Y. Woon, S. H. Chen, Y. L. Liu, S. M. He, C. Y. Su, M. Ota, S. Egashira, A. Morace, Y. Sakawa, Y. Abe, H. Habara, R. Kodama, L. N. K. Döhl, N. Woolsey, M. Koenig, H. S. Kumar, N. Ohnishi, M. Kanasaki, T. Asai, T. Yamauchi, K. Oda, Ko. Kondo, H. Kiriyama and Y. Fukuda, "Robustness of large-area suspended graphene under interaction with intense laser," *Sci. Rep.*, **12**, 2346 (2022).
- [29] O. Lundh, F. Lindau, A. Persson and C. G. Wahlström, "Influence of shock waves on laser-driven proton acceleration," *Phys. Rev. E*, **76**, 026404 (2007).
- [30] C. Thauray, F. QuéRé, J. P. Geindre, A. Levy, T. Ceccotti, P. Monot, M. Bougeard, F. Réau, P. d'Oliveira, P. Audebert, R. Marjoribanks and Ph. Martin, "Plasma mirrors for ultrahigh-intensity optics," *Nat. Phys.*, **3**, 424-429(2007).
- [31] F. Pegoraro and S. V. Bulanov, "Photon Bubbles and Ion Acceleration in a Plasma Dominated by the Radiation Pressure of an Electromagnetic Pulse," *Phys. Rev. Lett.*, **99**, 065002 (2007).

- [32] C. A. J. Palmer, J. Schreiber, S. R. Nagel, N. P. Dover, C. Bellei, F. N. Beg, S. Bott, R. J. Clarke, A. E. Dangor, S. M. Hassan, P. Hinz, D. Jung, S. Kneip, S. P. D. Mangles, K. L. Lancaster, A. Rehman, A. P. L. Robinson, C. Spindloe, J. Szerypo, M. Tatarakis, M. Yeung, M. Zepf and Z. Najmudin, "Rayleigh-Taylor Instability of an Ultrathin Foil Accelerated by the Radiation Pressure of an Intense Laser," *Phys. Rev. Lett.*, **108**, 225002 (2012).
- [33] Y. Wan, I. A. Andriyash, W. Lu, W. B. Mori and V. Malks. "Effects of the Transverse Instability and Wave Breaking on the Laser-Driven Thin Foil Acceleration," *Phys. Rev. Lett.*, **125**, 104801 (2020).
- [34] B. S. Paradkar and S. Krishnagopal. "Electron heating in radiation-pressure-driven proton acceleration with a circularly polarized laser," *Phys. Rev. E*, **93**, 023203 (2016).
- [35] J. W. Yoon, Y. G. Kim, I. W. Choi, H. W. Lee, S. K. Lee, C. H. Nam and Y. G. Kim, "Realization of laser intensity over 10^{23} W/cm²," *Optica* **8**(5): 630(2021).
- [36] S. M. Weng, M. Murakami, P. Mulser and Z. M. Sheng, "Ultra-intense laser pulse propagation in plasmas: from classic hole-boring to incomplete hole-boring with relativistic transparency," *New J. Phys.* **14**, 063026 (2012).
- [37] M. Grech, S. Skupin, A. Diaw, T. Schlegel and V. T. Tikhonchuk. "Energy dispersion in radiation pressure accelerated ion beams," *New J. Phys.* **13**, 123003(2011).
- [38] A. P. L. Robinson, P. Gibbon, M. Zepf, S. Kar, R. G. Evans and C. Bellei, "Relativistically correct hole-boring and ion acceleration by circularly polarized laser pulses," *Plasma Phys. Control. Fusion* **51**, 024004 (2009).
- [39] A. Pukhov and J. Meyer-ter-Vehn. "Laser hole boring into overdense plasma and relativistic electron currents for fast ignition of ICF targets," *Phys. Rev. Lett.* **69**, 3052 (1997).
- [40] T. P. Yu, A. Pukhov, G. Shvets and M. Chen, "Stable laser-driven proton beam acceleration from a two-ion-species ultrathin foil," *Phys. Rev. Lett.* **105**, 065002 (2010).
- [41] B. Qiao, M. Zepf, M. Borghesi and M. Geissler, "Stable GeV Ion-Beam Acceleration from Thin Foils by Circularly Polarized Laser Pulses," *Phys. Rev. Lett.* **102**, 145002(2009).
- [42] M. Chen, A. Pukhov and T. P. Yu, "Enhanced collimated GeV monoenergetic ion acceleration from a shaped foil target irradiated by a circularly polarized laser pulse," *Phys. Rev. Lett.* **103**, 024801 (2009).
- [43] T. D. Arber, K. Bennett, C. S. Brady, A. L. Douglas, M. G. Ramsay, N. J. Sircombe, P. Gillies, R. G. Evans, H. Schmitz, A. R. Bell and C. P. Ridgers, "Contemporary particle-in-cell approach to laser-plasma modelling," *Plasma Phys. Control. Fusion* **57**, 113001 (2015).
- [44] S. V. Bulanov, T. Zh. Esirkepov, M. Kando, F. Pegoraro, S. S. Bulanov, C. G. R. Geddes, C. B. Schroeder, E. Esarey and W. P. Leemans. "Ion acceleration from thin foil and extended plasma targets by slow electromagnetic wave and related ion-ion beam instability," *Phys. Plasmas*. **19**, 103105 (2012).
- [45] V. B. Berestetskii, E.M. Lifshitz, and L. P. Pitaevskii, "Quantum Electrodynamics," (Elsevier Butterworth-Heinemann, Oxford, 1982).
- [46] V. I. Ritus, "Quantum effects of the interaction of elementary particles with an intense electromagnetic field," *J. Sov. Laser Res.* **6**, 497 (1985).
- [47] V. N. Baier, V. Katkov, and V. M. Strakhovenko, "Electromagnetic Processes at High Energies in Oriented Single Crystals," (World Scientific, Singapore, 1998).
- [48] A. Di Piazza, C. Müller, K. Z. Hatsagortsyan, and C. H. Keitel, "Extremely high-intensity laser interactions with fundamental quantum systems," *Rev. Mod. Phys.* **84**, 1177?1228 (2012).
- [49] M. Tamburini, F. Pegoraro, A. Di Piazza, C. H. Keitel, and A. Macchi, "Radiation reaction effects on radiation pressure acceleration," *New J. Phys.* **12**, 123005 (2010).
- [50] J. Davis and G. M. Petrov, "Generation of GeV ion bunches from high-intensity laser-target interactions," *Phys. Plasmas* **16**, 023105 (2009).
- [51] Tanaka K. A., K. M. Spohr, D. L. Balabanski, S. Balascuta, L. Capponi, M. O. Cernaianu, M. Cuciuc, A. Cuceoanes, I. Dancus, A. Dhal, B. Diaconescu, D. Doria, P. Ghenuche, D. G. Ghita, S. Kisiov, V. Nastasa, J. F. Ong, F. Rotaru, D. Sangwan, P. A. Söderström, D. Stutman, G. Suliman, O. Tesileanu, L. Tudor, N. Tsoneva, C. A. Ur, D. Ursescu and N. V. Zamfir, "Current status and highlights of the ELI-NP research program," *Matter Radiat. Extremes* **5**, 024402 (2020).
- [52] Z. Gan, L. Yu, C. Wang, Y. Q. Liu, Y. Xu, W. Q. Li, S. Li, L. P. Yu, X. L. Wang, X. Y. Liu, J. C. Chen, Y. J. Peng, L. Xu, B. Yao, X. B. Zhang, L. R. Chen, Y. H. Tang, X. B. Wang, D. J. Yin, X. Y. Liang, Y. X. Leng, R. X. Li and Z. Z. Xu, "The Shanghai superintense ultrafast laser facility (SULF) project in Progress in Ultrafast Intense Laser Science XVI," (Springer International Publishing, Cham, 2021), p. 199.
- [53] C. Radier, O. Chalus, M. Charbonneau, S. Thambirajah, G. Deschamps, S. David, J. Barbe, E. Etter, G. Matras, S. Ricaud, V. Leroux, C. Richard, F. Lureau, A. Baleanu, R. Banici, A. Gradinariu, C. Caldararu, C. Capiteanu, A. Naziru, B. Diaconescu, V. Iancu, R. Dabu, D. Ursescu, I. Dancus, C. A. Ur, Kazuo, A. Tanaka and Nicolae Victor Zamfir, "10 PW peak power femtosecond laser pulses at ELI-NP," *High Power Laser Sci. Eng.* **10**, 03000e21 (2022).